Aeolian Research 16 (2015) 1–10

Contents lists available at ScienceDirect

Aeolian Research

journal homepage: www.elsevier.com/locate/aeolia

Regional transport of a chemically distinctive dust: Gypsum from White Sands, New Mexico (USA)

Warren H. White [a,*], Nicole P. Hyslop [a], Krystyna Trzepla [a], Sinan Yatkin [a], Randy S. Rarig Jr. [b], Thomas E. Gill [c], Lixin Jin [c]

[a] Crocker Nuclear Laboratory, University of California, Davis, United States
[b] PANalytical Incorporated, Westborough, MA, United States
[c] Department of Geological Sciences, University of Texas, El Paso, United States

ARTICLE INFO

Article history:
Received 18 August 2014
Revised 9 October 2014
Accepted 9 October 2014
Available online 18 November 2014

Keywords:
White Sands
Aerosols
Geogenic sulfate
Strontium
Gypsum

ABSTRACT

The White Sands complex, a National Monument and adjoining Missile Range in southern New Mexico, occupies the dry bed of an ice-age lake where an active gypsum dunefield abuts erodible playa sediments. Aerosols entrained from White Sands are sometimes visible on satellite images as distinct, light-colored plumes crossing the Sacramento Mountains to the east and northeast. The IMPROVE network (Interagency Monitoring of PROtected Visual Environments) operates long-term aerosol samplers at two sites east of the Sacramento range. In recent years a spring pulse of sulfate aerosol has appeared at these sites, eclipsing the regional summer peak resulting from atmospheric reactions of sulfur dioxide emissions. A significant fraction of this spring sulfate is contributed by gypsum and other salts from White Sands, with much of the sulfur in coarse particles and concentrations of calcium and strontium above regional levels. The increase in these gypsiferous species coincides with a drought following a period of above-average precipitation. White Sands and the IMPROVE samplers together provide a natural laboratory: a climatically sensitive dust source that is both well characterized and chemically distinct from its surroundings, with a signature that remains identifiable at long-term observatories 100–200 km downwind.

1. Introduction

Mineral dusts are poorly accounted for by existing models of atmospheric aerosols (e.g. Park et al., 2010; Huneeus et al., 2011). The particles entrained as aerosol are a non-random selection of the material present in the soil, and are not easily predicted from bulk soil composition (e.g. Bullard et al., 2007; Kok, 2011). The episodic and unconfined character of emissions complicates their characterization at the source, and the ubiquity of sources generally makes it hard to isolate specific source–receptor relationships for observation and study (e.g. Schutz and Sebert, 1987; Kavouras et al., 2009). This paper documents a "natural laboratory" where dust from a specific dry lake can be chemically identified in aerosols sampled more than 100 km downwind.

White Sands sits in the Tularosa Basin, whose geology is described by Fryberger (2001), Langford (2003), and KellerLynn (2012). A closed drainage within the northern Chihuahuan Desert, the Basin is a down-faulted block of earth's crust along the Rio Grande continental rift. The depression held a pluvial lake during the wetter climate of the most recent (Pleistocene) glaciation, and the lake collected mineral salts dissolved from exposed neighboring strata. As the waters evaporated in the more arid regional climate that followed, they left behind the gypsiferous deposits that characterize the area now known as White Sands. These Pleistocene deposits are easily identified in satellite imagery by their high albedo; as illustrated in Fig. 1, they appear as a distinctive white field in a landscape of desert browns. The darker north–south mountain ranges visible west (San Andreas) and east (Sacramento) of this field follow the faults delineating the Basin.

Much of White Sands is now protected by the National Park Service (NPS) as a National Monument, "the world's largest gypsum dunefield" (www.nps.gov/whsa/). Extensive research has been conducted on the hydrologic and aeolian processes shaping White Sands (e.g. Allmendinger, 1971; Schenk and Fryberger, 1988; Ghrefat et al., 2007; Kocurek et al., 2007; Langford et al., 2009; Szynkiewicz et al., 2010; Jerolmack et al., 2011). These investigations typically focus on the generation, saltation, and alteration of sand particles within the lake bed and dunefield, treating the

* Corresponding author at: Crocker Nuclear Laboratory, University of California, 1 Shields Avenue, Davis, CA 95616, United States. Tel.: +1 530 752 1213.
E-mail address: whwhite@ucdavis.edu (W.H. White).

http://dx.doi.org/10.1016/j.aeolia.2014.10.001
1875-9637/

escape of much smaller dust particles as minor leakage from the system of interest. White Sands' dust exports are harder to ignore in satellite imagery, where their distinctive whiteness can be easy to spot: Fig. 1 shows an example plume. The complex sedimentary environment of the White Sands places loose sand-sized sediments and finer-textured interdune and playa deposits adjacent to each other, facilitating dust generation through saltation and sandblasting-abrasion (Cahill et al., 1996). The alignment of prevailing springtime air flow with the orientation of the San Andres range creates a topographically-driven hydraulic enhancement of wind velocity in the Tularosa Basin, further enhancing dust emission (Novlan, 2011). White Sands has long been identified as a prototypical source and recurring "hotspot" of distinctive dust emissions (Savage, 1981; Breed and McCauley, 1986; Baddock et al., 2011).

The dominant springtime wind regime typically carries White Sands dusts over the Sacramento Mountains, to the White Mountain and/or Salt Creek Wilderness Areas to the north and east. A third Wilderness Area, Bosque del Apache to the north and west, is usually windward of the San Andreas Mountains and outside the White Sands plume. Atmospheric visibility is explicitly protected at all three of these "Mandatory Class I Federal Areas" (www.epa.gov/visibility/class1.html), so visibility-reducing fine particles are monitored at each as part of the Interagency Monitoring of PROtected Visual Environments (IMPROVE) program (http://vista.cira.colostate.edu/improve). The stars in Fig. 1 indicate the three sampler locations, and the star colors will distinguish the data from different samplers in subsequent plots. References to "background" (Bosque del Apache) and "downwind" (White Mountain and Salt Creek) measurements will be understood to assume a prevailing airflow similar to that in Fig. 1.

2. IMPROVE measurements

The IMPROVE monitoring program is described by Hand et al. (2011, Chapter 1). Standard operating procedures and details of quality assurance are collected at http://vista.cira.colostate.edu/improve/, and the precision of collocated measurements has been characterized by Hyslop and White (2008, 2009, 2011). Detailed site descriptions are available at http://views.cira.colostate.edu/web/SiteBrowser, and all ambient concentration data in this paper were downloaded from the public-access server at http://views.cira.colostate.edu/fed/DataWizard.

IMPROVE grew over time from a network of 36 sampling locations in early 1991 (Malm et al., 1994) to its current configuration of about 170. The three stations in Fig. 1 were installed during the years 2000–2001, and all were operating routinely by the start of 2002 (Fig. 2). Measurements are based on 24-h filter samples collected every third day (http://www.epa.gov/ttn/amtic/calendar.html). (The visible plume in Fig. 1 was imaged on one of the two-in-every-three idle days.) All sites report the same suite of measurements with the same sampling and analysis methods.

Each IMPROVE site employs four parallel sampling trains to collect particles for different measurements. Samples of fine particulate matter ($PM_{2.5}$, D_{aero} < 2.5 μm) are collected on three different filter media, and PM_{10} (D_{aero} < 10 μm) is collected on a fourth filter. $PM_{2.5}$ samples on appropriate media are analyzed for mass by weighing, elements by energy-dispersive X-ray fluorescence (XRF), anions by ion chromatography of deionized water extracts, and carbon by thermal–optical analysis; the PM_{10} sample is weighed, normally without any chemical analysis. The mass and elemental data are from samples collected on 25 mm PTFE membrane filters at 22.8 lpm, all analyzed by Crocker Nuclear Laboratory at the University of California, Davis. Elemental analysis through the 2010 sample year was performed on lab-built custom XRF systems whose multi-year consistency was characterized by Hyslop et al. (2012). Samples from 2011 and subsequent years were analyzed on commercial Epsilon-5 XRF systems from

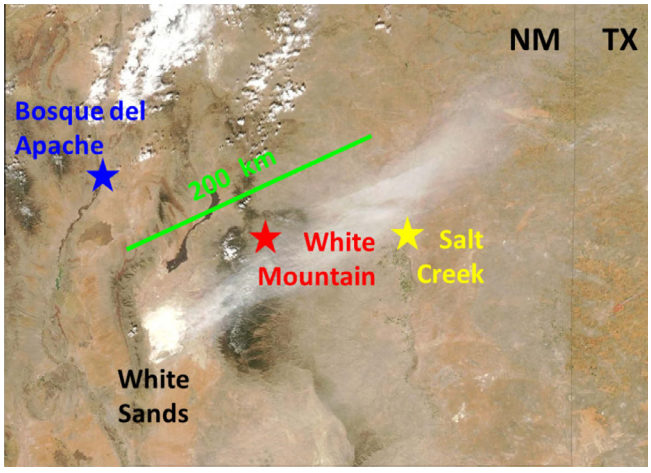

Fig. 1. A dust plume from White Sands blows north-eastward toward the New Mexico–Texas border. NASA's MODIS Aqua captured this natural-color image on February 28, 2012 (http://earthobservatory.nasa.gov/NaturalHazards/view.php?id=77294). The green distance scale is aligned with the mean sand-transport vector calculated from 1964–2008 wind data by Jerolmack et al. (2011). The white patches to the north are clouds. (For interpretation of the references to color in this figure legend, the reader is referred to the web version of this article.)

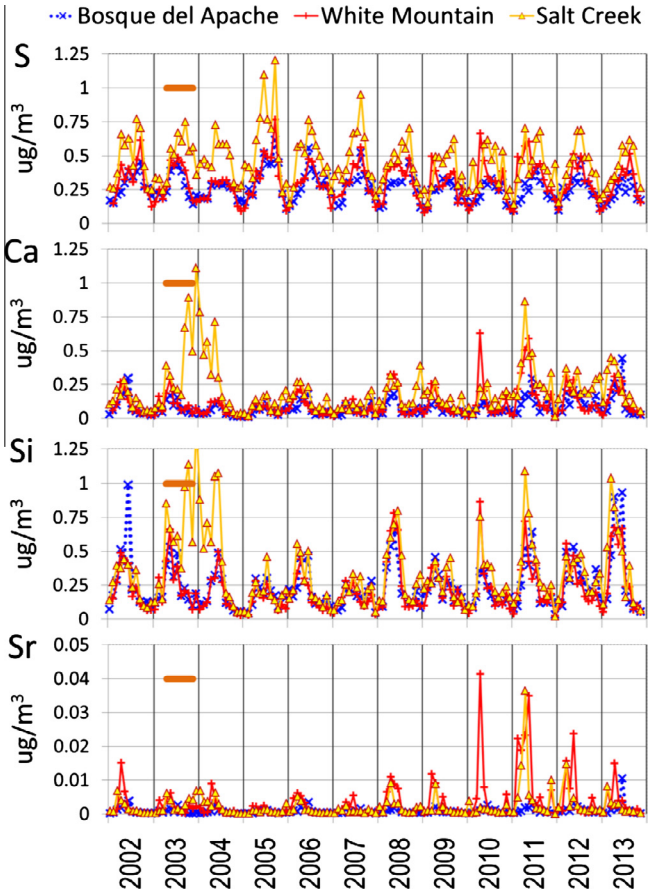

Fig. 2. Monthly mean concentrations of fine particulate matter (D_{aero} < 2.5 μm) at the three sampling sites in Fig. 1. Months with fewer than six valid samples at a site are not plotted. A period of levee construction near the Salt Creek sampler is indicated by a horizontal bar; contemporary field notes associated the 2003 onset of unusual dust levels at Salt Creek with the start of this local activity.

PANalytical with three-dimensional polarizing optics and a series of seven secondary targets. The introduction of new instrumentation had negligible effects for the relationships highlighted here (Fig. SI-1 of Supplemental Information).

The characteristic mineral of White Sands is gypsum, which in its pure form is a hydrate of calcium sulfate ($CaSO_4{\cdot}2H_2O$). Calcium and sulfur are both well characterized by IMPROVE measurements, and both contribute substantially to $PM_{2.5}$ throughout the U.S. southwest (Fig. SI-2 of Supplemental Information). Their presence in the same $PM_{2.5}$ sample cannot be interpreted *per se* as evidence of gypsum, though, as both elements have other major sources. Most $PM_{2.5}$ S is attributed to anthropogenic SO_2 emissions (Langner et al., 1992), converted through a series of atmospheric reactions to a haze aerosol of ammonium sulfates (Hand et al., 2011, Chapter 2). Most Ca in continental $PM_{2.5}$ is attributed to soil dust (Hand et al., 2011, Chapter 2), and Ca appears in soils predominantly as carbonates and silicates (Eberl and Smith, 2009).

Strontium, grouped with Ca in the periodic table, is one of the better-measured IMPROVE trace elements. Gypsum deposits commonly contain some Sr, both as a substituent for Ca in the gypsum lattice and as a constituent of celestite ($SrSO_4$), a separate mineral phase (Playa and Rosell, 2005). Like Ca, Sr has sources other than gypsum: it is a recognized marker for sea salt aerosols (Lowenthal and Kumar, 2006; White, 2008), and is also found in carbonates and other soil minerals (Capo and Chadwick, 1999). Fig. 2 shows that $PM_{2.5}$ Sr concentrations peak sharply during the spring dust months at White Mountain and Salt Creek, but not at Bosque del Apache. The difference between its behavior at the background and downwind sites suggests that Sr is not a significant constituent of generic regional dust, and can be considered a marker for White Sands. This attribution is supported by the absence of Sr in the Si- and Ca-rich local dusts associated with the 2003 levee construction at Salt Creek.

Fig. 2 plots absolute elemental concentrations in the dimensions reported by IMPROVE, as the mass of element carried by fine particles within a reference volume of air at local atmospheric conditions. The right-hand panel of Fig. 3 plots elemental data as relative concentrations, showing the mass of element carried by a reference mass of fine particles. These relative concentrations are the dimensionless ratios of the (absolute) elemental concentrations obtained from XRF analysis to the (absolute) $PM_{2.5}$ mass concentrations obtained from gravimetric analysis, and are calculated only for samples with $PM_{2.5} \geqslant 5\ \mu g/m^3$. The resulting intensive description of IMPROVE $PM_{2.5}$ composition admits direct comparison with similarly intensive composition data from analyses of independently collected geochemical samples, such as the soils shown in the left-hand panel of Fig. 3. The distinction between concentration and composition data is a potential source of misunderstanding between soil and aerosol scientists, as discussed in Supplemental Information.

Fig. 3 highlights the exceptional abundance of Sr in spring $PM_{2.5}$ at White Mountain and Salt Creek. The right-hand panel displays the Sr and Ca compositions measured at all 173 IMPROVE sites during spring 2008–2013. Out of almost 10,000 samples with at least 5 $\mu g/m^3$ $PM_{2.5}$, just over 1% had Sr contents above 1 mg/g combined with Sr/Ca ratios higher than in seawater. Of these 108 Sr-rich samples, 74 were from White Mountain or Salt Creek; the only other samplers collecting more than one or two during this period were at distant Death Valley in California (11 Sr-rich samples) and Great Basin in Nevada (4 Sr-rich samples). No comparable "finger" of high Sr contents and Sr/Ca ratios is present in the left-hand panel, which summarizes the Sr and Ca compositions from an extensive soil sampling program by the U.S. Geological Survey (Smith et al., 2013).

None of the USGS soil samples were collected from the high-albedo gypsum deposits of White Sands, but Fig. 3 shows similarly unremarkable Sr and Sr/Ca levels for unconsolidated dune sand analyzed as part of the present study. This sand was ground to powder and analyzed by PANalytical Inc. (Westborough, MA) using the standardless analysis software package "Auto Quantify" on an Epsilon-5. Collected at the fence line of the National Monument, our sand sample is not representative of other White Sands microenvironments such as playa crusts and interdune areas. A more general point, to be elaborated in a subsequent section, is that fine particles entrained as dust and sampled by IMPROVE need not be chemically representative of all particles present in any bulk sample of soil or sand.

3. Dust element balance

This section will demonstrate that dusts downwind of White Sands can be represented as a varying mix of two chemically distinct fractions. One end-member of the mix is recognizable as

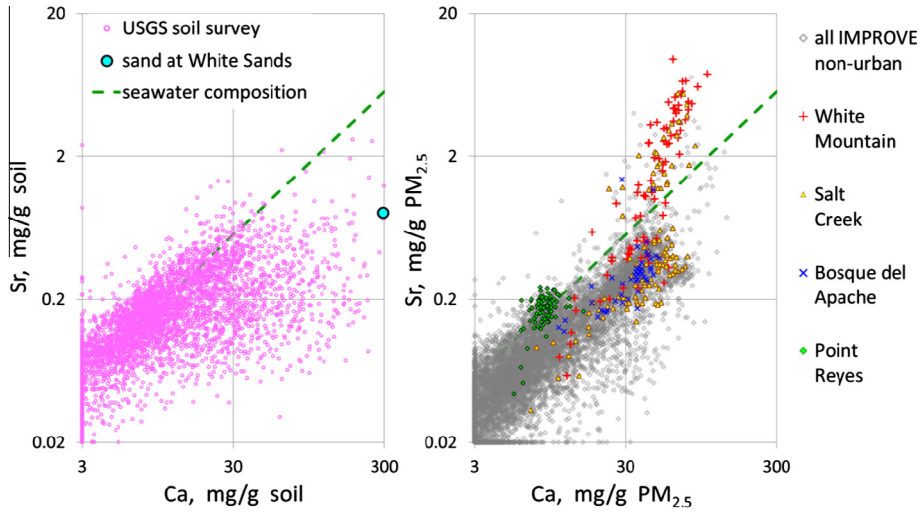

Fig. 3. Strontium and calcium contents of soil and fine-particle samples. The Sr/Ca ratio in seawater (Millero, 2004, Table 1) is indicated for later reference. Off-scale points are plotted at the appropriate boundaries. (left) All surface (0–5 cm) soil samples from a geochemical survey of 4857 sites across the conterminous United States (Smith et al., 2013). A sample of dune sand collected in the present study is also plotted. (right) All 9151 $PM_{2.5}$ samples with at least 5 $\mu g/m^3$ total mass from 173 non-urban IMPROVE sites during March, April, and May of 2008–2013. Samples from three sites near White Sands (Fig. 1) are highlighted, along with those from a seacoast site (Point Reyes National Seashore, California) for comparison.

r	Al	Si	K	Fe	Mn	Ti	S	Na	Mg	Cl	Ca	Sr
Al	1	0.97	0.96	0.97	0.94	0.96	0.54	0.45	0.66	0.53	0.76	0.59
Si	0.97	1	0.96	0.94	0.92	0.91	0.63	0.61	0.70	0.67	0.86	0.70
K	0.96	0.96	1	0.98	0.97	0.95	0.69	0.48	0.77	0.64	0.84	0.70
Fe	0.97	0.94	0.98	1	0.97	0.99	0.54	0.37	0.69	0.53	0.76	0.59
Mn	0.94	0.92	0.97	0.97	1	0.96	0.55	0.38	0.71	0.54	0.78	0.61
Ti	0.96	0.91	0.95	0.99	0.96	1	0.51	0.32	0.65	0.47	0.71	0.54
S	0.54	0.63	0.69	0.54	0.55	0.51	1	0.68	0.70	0.75	0.78	0.75
Na	0.45	0.61	0.48	0.37	0.38	0.32	0.68	1	0.55	0.86	0.77	0.79
Mg	0.66	0.70	0.77	0.69	0.71	0.65	0.70	0.55	1	0.83	0.89	0.89
Cl	0.53	0.67	0.64	0.53	0.54	0.47	0.75	0.86	0.83	1	0.91	0.94
Ca	0.76	0.86	0.84	0.76	0.78	0.71	0.78	0.77	0.89	0.91	1	0.94
Sr	0.59	0.70	0.70	0.59	0.61	0.54	0.75	0.79	0.89	0.94	0.94	1

Fig. 4. Inter-element correlations in $PM_{2.5}$ concentrations from 2008–2013 samples at White Mountain ($n = 661$). Correlations involving potassium exclude 153 samples with elemental carbon concentrations suggestive of a contribution by wood smoke (EC $\geqslant$ 0.1 μg/m^3). Values above 0.9 (0.8) are shaded (bolded) to highlight clusters of associations.

a generic regional dust rich in silicate minerals, and will be referred to as "background" dust. The other end-member exhibits an overall Sr/Ca ratio exceeding that of seawater, and is interpreted as a blend of gypsum with celestite, halite, and other evaporite minerals.

Fig. 4 shows inter-element correlations observed in recent years at White Mountain during the spring dust season. The selected elements are ordered to reveal the "two-factor" pattern of their covariance. Al, Si, K, Fe, and other elements representative of rock-forming minerals all correlate tightly with each other, as we would expect from a silicate-dominated dust background of uniform composition and varying concentration. Conversely, Ca, Sr and Cl correlate more tightly with each other than with any of the former group, suggesting a different shared source of variability. The White Sands gypsum deposits are an obvious source for both Ca and Sr, as discussed earlier. The White Sands deposits also include halite and other evaporites, accounting for the association of Cl with Ca and Sr. The observed correlations of Na and Mg with other elements of the evaporite group are probably depressed by the effects of measurement error, as these two lighter elements are more difficult to quantify by XRF. The association of

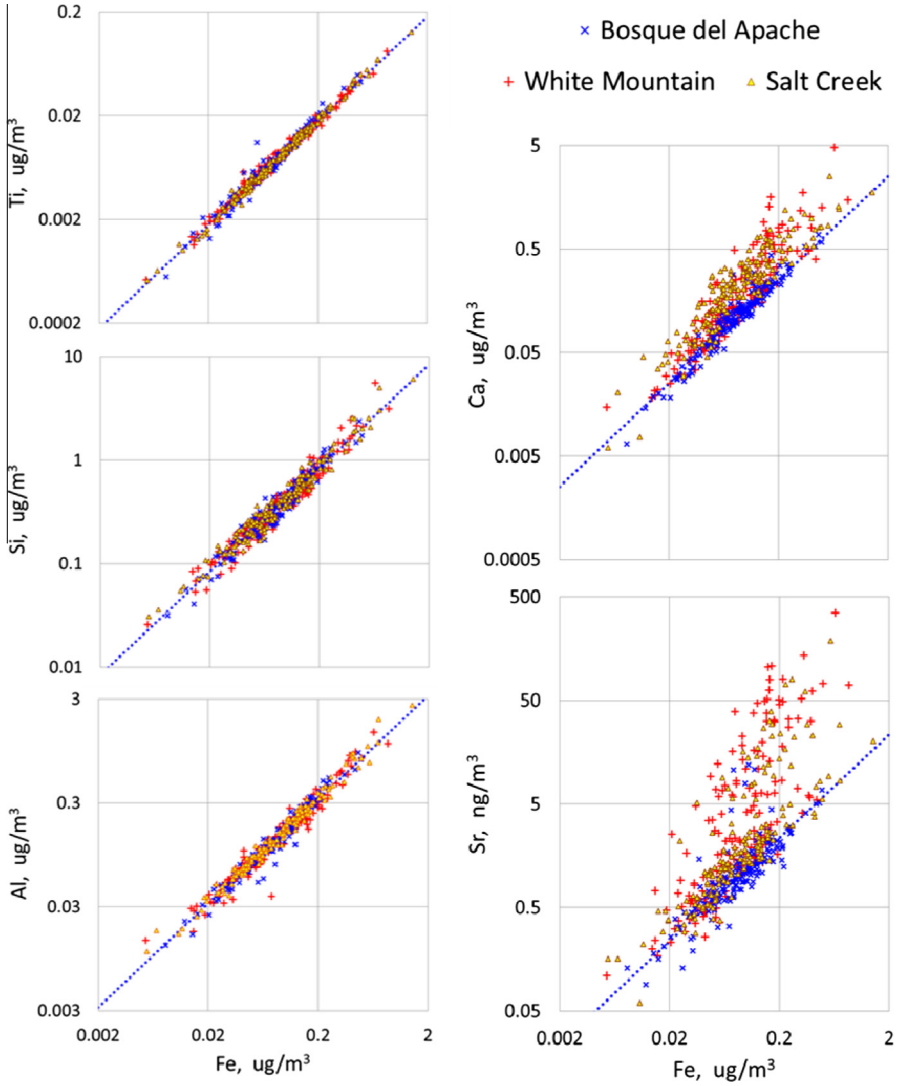

Fig. 5. Spring (March, April, May) $PM_{2.5}$ samples during 2008–2012 from three sites near White Sands. Dotted blue lines indicate the median elemental mass ratios at Bosque del Apache: Al/Fe = 1.62, Si/Fe = 4.2, Ti/Fe = 0.89, Ca/Fe = 1.27, and Sr/Fe = 0.0117. These ratios are assumed to indicate the average composition of crustal silicates at all three sites.

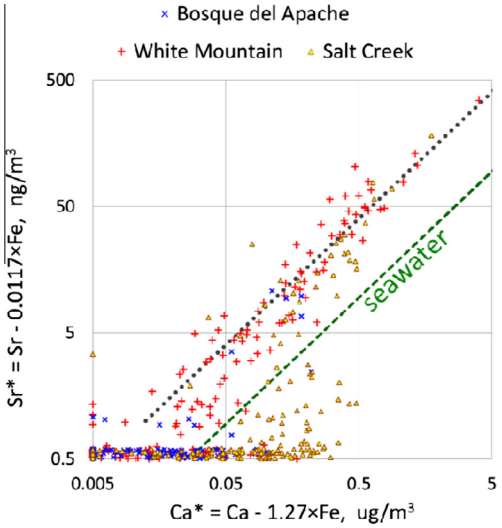

Fig. 6. Estimates of evaporite strontium and calcium for the spring 2008–2013 samples shown in Fig. 5. Below-scale values are plotted at the boundaries, with jittering for better visibility. The dashed green line indicates the strontium/calcium mass ratio in seawater (Millero, 2004, Table 1). The unlabeled dotted line ($Sr^* = 0.08 \times Ca^*$) is fit by eye to samples with elevated strontium. (For interpretation of the references to colour in this figure legend, the reader is referred to the web version of this article.)

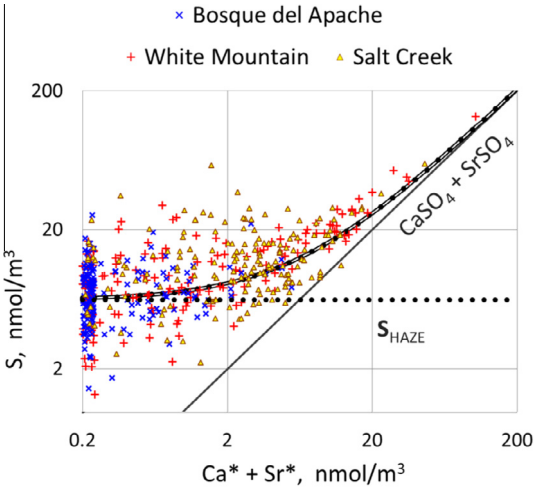

Fig. 7. Relationship of observed sulfur to the evaporite strontium and calcium estimates shown in Fig. 6. A representative regional S background of 0.2 μg/m^3 = 6.2 nmol/m^3 is suggested by the dotted line. Total sulfur expected in the presence of this background is indicated by the curve. Below-scale values are plotted at the boundary, with jittering for better visibility.

gypsiferous elements with sulfur is obscured by the large, and independently varying, contribution of anthropogenic emissions to the total S that is measured.

Figs. 5 and 6 depict springtime dusts at all three Fig. 1 sites in terms of the two factors identified in the element correlations at White Mountain. Fig. 5 cross-plots five different elements against iron, which is chosen for the common abscissa as the most reliably determined of the six. The three left-hand plots display the tight correlations noted in Fig. 4 among elements we attribute primarily to silicates. The relative proportions of these elements are effectively identical at all three sites, suggesting a fraction that can be considered a chemically homogeneous component of regional background dust. The two right-hand plots show much looser associations with iron for two of the gypsiferous elements. There are minimum observed Ca and Sr concentrations that are proportional to observed iron concentrations, and most samples from Bosque del Apache approach these minimum proportions. We interpret these minima as the Ca and Sr content of the regional dust background. At White Mountain and Salt Creek, the sites more often downwind of White Sands, samples typically exhibit Ca and Sr contents well in excess of the background minima indicated by their iron content. We interpret this excess as the evaporite increment contributed by White Sands.

Our interpretation of Fig. 5 implies that the excesses of Ca and Sr above their iron-related minima should correlate with each other, in a proportion reflective of the evaporite dust. Fig. 6 cross-plots these excesses, subtracting background contributions based on the median ratios Ca/Fe and Sr/Fe measured in samples from Bosque del Apache. Calculated as differences between two measurements, $Ca^* = Ca - 1.27 \times Fe$ and $Sr^* = Sr - 0.0117 \times Fe$, the estimated evaporite contributions have large relative uncertainties at low concentrations. Above 1–3 ng/m^3 excess strontium, however, Ca* and Sr* track each other reasonably well, especially at White Mountain. The relationship implies a strontium/calcium ratio for evaporite dust that is well above marine values.

The evaporite sulfate that we expect to accompany Ca* and Sr* is masked at low dust concentrations by the substantial regional background of anthropogenic sulfate. Fig. 7 reveals the evaporite contribution as a lower bound that becomes increasingly evident as evaporites account for increasing amounts of observed total sulfur. To aid interpretation, a curve shows the observable sum of evaporite sulfur with a constant anthropogenic background, S_{HAZE}.

The relationships depicted in Figs. 5–7 allow us to estimate White Sands' contribution to Ca and S concentrations at White Mountain. Fig. 8 extrapolates, to all months and all years, relationships based on analysis of only March–May data from 2008–2013. "Background" Ca attributable to regional dust is estimated from Fe as $1.27 \times Fe$ (Fig. 5). Gypsiferous S is estimated stoichiometrically from $Ca^* = Ca - 1.27 \times Fe$ and $Sr^* = Sr - 0.0117 \times Fe$ (Fig. 7). Gypsiferous Ca is estimated, independently of the Ca measurement, as $Sr^*/0.08$ when $Sr^* > 1$ ng/m^3 and zero otherwise (Fig. 6). The elemental markers (Fe, Ca, Sr) needed for these estimates are all measured at White Mountain, and the measured Ca both here and at Salt Creek is well approximated as the sum of estimated background and gypsiferous contributions. We have no White Mountain tracer for anthropogenic haze S, but it is not unreasonable to suppose that regional haze measured at Bosque del Apache is representative also of White Mountain. With this assumption, our attributions reproduce the seasonal shift in peak sulfur concentrations observed at White Mountain in recent years. The sulfur balance is less satisfactory at Salt Creek (not shown), which is more exposed to extraneous S emissions from petroleum production and industrial activity to the south and east. As was evident in Fig. 2, Salt Creek S concentrations run well above those at Bosque del Apache and White Mountain.

Fig. 8 is wholly based on routine IMPROVE data for $PM_{2.5}$, the fraction of particulate matter carried by particles less than 2.5 μm in aerodynamic diameter. Regulatory monitoring programs in the United States focus on $PM_{2.5}$ as the particle size fraction most relevant to visibility (Malm et al., 1994) and human health (White, 2009), but larger particles carry most of the suspended particle mass in the arid southwest (Neff et al., 2013). The White Mountain sampler shelter acts as a settling chamber for suspended particles of all sizes, which have accumulated over time in loess-like deposits. X-ray and laser diffraction analyses by the authors at UTEP show the collected material to be more than 40% gypsum, with more than 70% of the mass in particles too large for capture in PM_{10} samples.

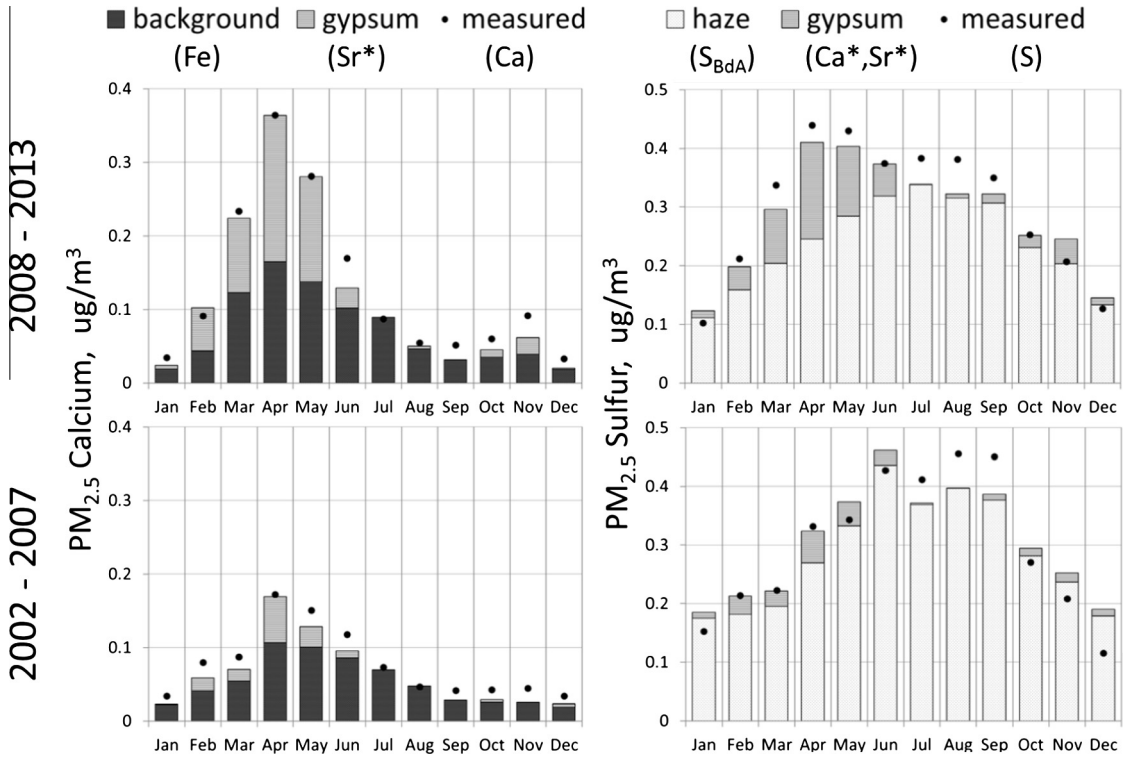

Fig. 8. Estimated contributions of gypsiferous dust to White Mountain $PM_{2.5}$. The elements used to estimate different components, as described in the text, are indicated in parentheses.

Fig. 9 presents PM_{10} sulfur concentrations from XRF analyses performed on a limited selection of routine samples from White Mountain and two other sites. As part of an unrelated investigation, 29 of these samples collected in 2011 at White Mountain and the North Absaroka (Wyoming) and Wheeler Peak (New Mexico) Wilderness Areas were analyzed by XRF. An additional 24 White Mountain samples from 2012 were then analyzed to support the present study. The majority of all 53 analyses show sulfur contents for the $PM_{2.5}$ and PM_{10} samples that are indistinguishable from each other, indicating an absence of sulfur in coarse particles ($2.5\ \mu m < D_{aero} < 10\ \mu m$). Such agreement reflects the generally fine particle size of secondary sulfate aerosol in arid climates (Wilson and McMurry, 1981; Sanchez et al., 2000), and is observed elsewhere as well. Coarse-particle sulfate concentrations were consistently found to be negligible in a more comprehensive special study lasting a full year at 9 other IMPROVE sites (Malm et al., 2007).

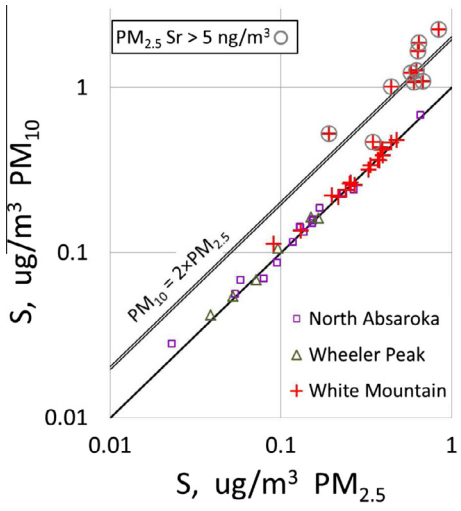

Fig. 9. Comparison of $PM_{2.5}$ S with PM_{10} S in selected samples from three IMPROVE sites. Samples with elevated concentrations of $PM_{2.5}$ Sr are highlighted as indicated.

Fig. 9 shows coarse particles to contribute much of the sulfur in about one-third of the PM_{10} samples analyzed at White Mountain. The samples with the most coarse-particle sulfur are all rich in strontium, and all but one are from the "spring" months March–May. In light of the source–receptor relationships already established, it seems reasonable to attribute all coarse-particle S at White Mountain to gypsum. Combined with the fine-particle contribution based on Ca* and Sr*, this implies that gypsiferous dust accounts for fully 80% of the total PM_{10} S in the 10 circled samples of Fig. 9.

4. Discussion

A disproportionate fraction of both regional and global dust emissions is associated with the dry stages of ephemeral water bodies (Sinclair, 1969; Baddock et al., 2011; Ginoux et al., 2012). Intermittent inundation of these topographic depressions brings supplies of silt and salts that are then left behind on desiccated playas as unconsolidated fine sediment and evaporite crusts. Such a playa in the Tularosa Basin is the ephemeral Lake Lucero, which has alternated between inundation and desiccation several times since 2002. The Basin as a whole still functions as a natural reservoir, the arid post-glacial climate now holding the water table's capillary fringe generally at or just below the surface (Fryberger, 2001; Scheidt et al., 2010). The level and salinity of the shallow groundwater vary in space and time, shaping patterns of cementation (Schenk and Fryberger, 1988) and vegetation (Langford et al., 2009). Evaporation of saline groundwater through playa sediments in similar settings has been observed to produce "fluffy" evaporite

formations that are particularly vulnerable to wind erosion (Reynolds et al., 2007). This section will consider hydrologic factors as possible explanations for features in the downwind aerosol.

4.1. Strontium enrichment

Observational (Stewart, 1964; Rosell et al., 1998) and experimental (Ichikuni and Musha, 1978; Kushnir, 1980) studies suggest the composition of seawater as a rough upper limit on the Sr/Ca ratio in gypsum. Fig. 3 shows that IMPROVE $PM_{2.5}$ samples at White Mountain and Salt Creek often have Sr/Ca ratios well above the 19 g/kg value for seawater at normal salinity (Millero, 2004). Fig. 6 suggests a typical Sr^*/Ca^* ratio of about 80 g/kg, implying that most of the evaporite Sr did not coprecipitate with Ca as part of the gypsum lattice but instead crystalized separately. The discrete mineral phase celestite ($SrSO_4$) is in fact a common contaminant of, or replacement for, natural gypsum (West, 1973; Playa and Rosell, 2005). Warren (2006; pp. 548–9) lists a variety of geochemical processes known to produce strontium-rich brines capable of precipitating celestite. Hogan et al. (2007) reported Sr/Ca ratios exceeding 25 g/kg in Tularosa Basin brines and groundwaters, and Bein and Dutton (1993) reported brines saturated with respect to celestite in hydrostratigraphic units just east of the region studied here. The Sr enrichment of White Mountain and Salt Creek aerosols adds to their chemical distinctiveness, and nicely highlights the limits of bulk soil chemistry in accounting for dust aerosol composition. It is not, however, essential to our identification and quantification of a gypsiferous contribution; Sr is a minor aerosol constituent even downwind of White Sands. At the mass ratio Sr/Ca = 0.08 suggested by Fig. 6, $SrSO_4$ accounts for only $\frac{40.1}{87.6} \times 0.08 < 4\%$ of the mineral sulfate mass.

The dusts sampled as $PM_{2.5}$ or PM_{10} at White Mountain and Salt Creek contain only the smallest of the particles mobilized from White Sands, so any tendency of celestite to precipitate as smaller grains would increase Sr/Ca ratios in dusts over those in the parent deposit. Kushnir (1980) showed experimentally that kinetic factors affect gypsum's Sr content: faster precipitation rates and more concentrated brines produce higher Sr/Ca ratios, with a negative

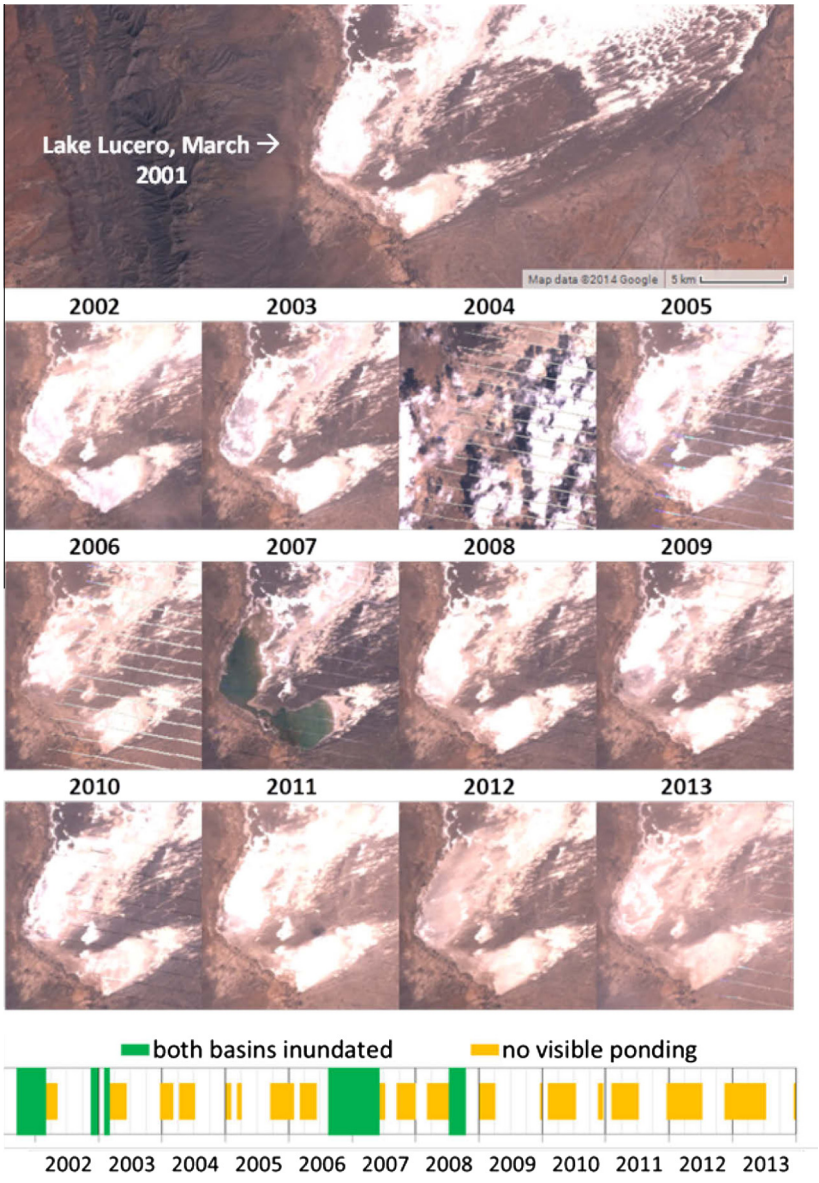

Fig. 10. Landsat 7 views of the ephemeral Lake Lucero during early spring. Each frame shows detail from a 32-day raw composite produced by Google Earth Engine (https://earthengine.google.org) for March 5–6 to April 6–7 of the indicated year. Lake Lucero is at the southern tip of the white deposits visible in Fig. 1. Unclassified periods in the bottom timeline correspond to composites showing limited wet areas or obscured by cloud cover.

correlation between Sr concentration and crystal size. Ham (1962; pp. 146–7) reported the ubiquitous presence of celestite micro-crystals in western Oklahoma gypsum deposits formed by hydration of anhydrite, a process yielding Sr-rich brines. Hamdi-Aissa et al. (2004) reported needle-like micro-crystals of celestite on the periphery of gypsum crystals from a playa in the Algerian Sahara. Glamoclija et al. (2012) recently found micron-sized precipitates of celestite associated with interdune biofilms at White Sands, likely resulting from microbial activity. These observations illustrate various mechanisms potentially differentiating the size distributions of precipitated strontium sulfate and calcium sulfate mineral grains.

4.2. Interannual variations

The division of years for the dust budgets in Fig. 8 was chosen to highlight the sustained increase, starting in 2008, in Sr-rich dust concentrations at White Mountain and Salt Creek (cf. Fig. 2). A variety of factors could potentially contribute to increased evaporite dust levels, including changes in wind patterns, human activity, and soil conditions (Brahney et al., 2013), but here we will focus on hydrology. The availability of playa sediments can be sensitive to water-table depth (Pelletier, 2006; Reynolds et al., 2007), but this factor does not seem to be routinely monitored. Soil moisture, which can be remotely sensed as a function of apparent thermal inertia, is another indicator of sediment availability. Using data from the ASTER satellite radiometer, Scheidt et al. (2010) produced high-resolution maps of soil moisture and threshold wind velocity patterns in White Sands National Monument. The data requirements of the recovery technique – near-coincident and cloud-free day and night passes over White Sands, by a satellite with a repeat time of about 16 days – limited its application to 7 irregularly spaced dates between 2002 and April 2008, when ASTER's detectors began rapidly to degrade. Much the driest of the 7 retrievals was the last, in March 2008, days before "the largest dust emission event at White Sands in decades."

Lake Lucero's status provides an alternative indication of the Tularosa Basin's hydrologic state. Whether it is inundated or desiccated is often evident in archived Landsat imagery, as illustrated in Fig. 10. A subjective assessment (by WHW) of monthly composites from the years 2002–2013 is summarized in the timeline at the bottom of this figure. Spring is normally the season with the year's driest surface soils, and the 2006–2007 inundation was the only sustained spring flooding observed since IMPROVE monitoring began. The 2006 "monsoon" was as singular as the inundation it left in its wake; accounts of its impact on a nearby metropolitan area are given by Gill et al. (2009) and Rogash et al. (2009). The White Sands weather station (GHCND:USC00299686) received 24 cm precipitation in the single month of August 2006 and 16 cm more in September and October 2006, after averaging annual totals of 20 cm during the previous five calendar years. The dissolution and recrystallization of White Sands salts caused by the massive influx and subsequent evaporation of fresh water seems likely to have helped shape spring dust emissions in the years following 2007. Other factors have also played important roles, of course; drought conditions in much of the region during much of 2011–2013 were categorized as "extreme" or "exceptional" by the United States Drought Monitor (http://droughtmonitor.unl.edu).

5. Summary and conclusions

IMPROVE aerosol samplers in the White Mountain and Salt Creek Wilderness Areas periodically collect distinctive fine and coarse dust that appears to originate 100–200 km upwind, in the White Sands gypsum deposits. $PM_{2.5}$ Ca concentrations at White Mountain and Salt Creek are high relative to other crustal elements (e.g. Al, Si, Ti, Fe) in the same samples (Fig. 5), and are also high relative to Ca at Bosque del Apache, a nearby site that is shielded from White Sands by topography and prevailing weather patterns. The highest $PM_{2.5}$ Ca concentrations at the downwind sites are invariably accompanied by elevated S concentrations (Fig. 7), and analyses of selected PM_{10} samples from White Mountain show large concentrations of coarse S-containing particles (Fig. 9). Gypsiferous aerosols at White Mountain and Salt Creek are further distinguished by Sr concentrations and Sr/Ca mass ratios rarely if ever seen elsewhere in the IMPROVE network (Fig. 3). The Sr signature became stronger in the dry years following an unusually prolonged inundation of White Sands (Figs. 2 and 10). Strontium/calcium ratios observed in fine dust exceed those in sea salt aerosols or regional soils (Fig. 3), and elevated Sr and Ca concentrations co-occur in the same subset of samples (Fig. 6).

Much of the White Sands source area remains under the protection of the National Park Service and accessible to on-site study and characterization. The IMPROVE program plans to continue monitoring at the White Mountain and Salt Creek receptor locations into the foreseeable future. The downwind aerosol's response to future climatic and hydrologic variations will not only supply a steadily accumulating pool of observations, but will also support prospective testing of hypotheses and models that interested researchers develop to account for them. The "natural laboratory" remains open for further observation and experiment.

Acknowledgments

This analysis was supported by National Park Service funding through Cooperative Agreement P11AC91283 with the University of California at Davis, and the NOAA Educational Partnership Program with Minority Serving Institutions (EPP/MSI) through cooperative agreements NA17AE1625 and NA17AE1623 with the University of Texas at El Paso.

Appendix A. Supplementary material

The dimensions of concentration (particle mass per sampled air volume) in which IMPROVE data are reported may be unfamiliar to some readers. Geochemists are more likely to work with "compositional data", vectors of non-negative proportions that sum to unity (Aitchison, 1986). It has been argued that "almost all data presented in environmental sciences are compositional" (Filzmoser et al., 2010). This perspective is appropriate to sampling procedures that collect a predetermined amount of specimen, so that "compositional data are parts of a whole which only give relative information" (Filzmoser et al., 2009). The constraint that parts must sum to the whole "has severe consequences for bivariate statistical analysis ... and the information contained in scatterplots must be used and interpreted differently" (Filzmoser et al., 2010). An example of these consequences in an aerosol context was given by Andrews et al. (2000, Appendix). Such concerns do not apply to our analysis of IMPROVE concentration data, because the particle mass and sampled air volume are incommensurable and the species concentrations do not sum to a unit "whole". The amount of particulate specimen collected on a filter over a 24h sampling interval is not predetermined, and instead carries information about atmospheric conditions that is otherwise unknown to the experimenter. IMPROVE concentration data are "open" rather than "closed", in the terminology of Aitchison

(1986), and are properly plotted and analyzed in the usual euclidean-space framework. Supplementary data associated with this article can be found, in the online version, at http://dx.doi.org/10.1016/j.aeolia.2014.10.001.

References

Aitchison, J., 1986. The Statistical Analysis of Compositional Data. Chapman and Hall, London.

Allmendinger, R.J., 1971. Hydrologic Control over the Origin of Gypsum at Lake Lucero, White Sands National Monument, New Mexico. M.S. Thesis, New Mexico Institute of Mining and Technology, Socorro.

Andrews, E., Saxena, P., Musarra, S., Hildemann, L.M., Koutrakis, P., McMurry, P.H., Olmez, I., White, W.H., 2000. Concentration and composition of atmospheric aerosols from the 1995 SEAVS experiment and a review of the closure between chemical and gravimetric measurements. J. Air Waste Manage. Assoc. 50, 648–664.

Baddock, M.C., Gill, T.E., Bullard, J.E., Acosta, M.D., Rivera Rivera, N.I., 2011. Geomorphology of the Chihuahuan Desert based on potential dust emissions. J. Maps 2011, 249–259.

Bein, A., Dutton, A.R., 1993. Origin, distribution, and movement of brine in the Permian Basin (U.S.A.): a model for displacement of connate brine. Geol. Soc. Am. Bull. 105, 695–707.

Brahney, J., Ballantyne, A.P., Sievers, C., Neff, J.C., 2013. Increasing Ca^{2+} deposition in the western US: the role of mineral aerosols. Aeolian Res. 10, 77–87.

Breed, C.S., McCauley, J.F., 1986. Use of dust storm observations on satellite images to identify areas vulnerable to severe wind erosion. Clim. Change 9, 243–258.

Bullard, J.E., Mctainsh, G.H., Pudmenzky, C., 2007. Factors affecting the nature and rate of dust production from natural dune sands. Sedimentology 54, 169–182.

Cahill, T.A., Gill, T.E., Reid, J.S., Gearhart, E.A., Gillette, D.A., 1996. Saltating particles, playa crusts and dust aerosols at Owens (dry) Lake, California. Earth Surf. Proc. Land. 21, 621–639.

Capo, R.C., Chadwick, O.A., 1999. Sources of strontium and calcium in desert soil and calcrete. Earth Planet. Sci. Lett. 170, 61–72.

Eberl, D.D., Smith, D.B., 2009. Mineralogy of soils from two continental-scale transects across the United States and Canada and its relation to soil geochemistry and climate. Appl. Geochem. 24, 1394–1404.

Filzmoser, P., Hron, K., Reimann, C., 2009. Univariate statistical analysis of environmental (compositional) data: problems and possibilities. Sci. Total Environ. 407, 6100–6108.

Filzmoser, P., Hron, K., Reimann, C., 2010. The bivariate statistical analysis of environmental (compositional) data. Sci. Total Environ. 408, 4230–4238.

Fryberger, S.G., 2001. Geological Overview of White Sands National Monument. <http://www.nature.nps.gov/geology/parks/whsa/geows/index.htm>.

Ghrefat, H.A., Goodell, P.C., Hubbard, B.E., Langford, R.P., Aldouri, R.E., 2007. Modeling grain size variations of aeolian gypsum deposits at White Sands, New Mexico, using AVIRIS imagery. Geomorphology 88, 57–68.

Gill, T.E., Collins, T.W., Novlan, D.J., 2009. Variable impacts and differential response to flash flooding in the *Paso del Norte* metroplex (El Paso, Texas, USA/Ciudad Juárez, Chihuahua, Mexico). American Meteorological Society Annual Meeting. <https://ams.confex.com/ams/pdfpapers/148065.pdf>.

Ginoux, P., Prospero, J.M., Gill, T.E., Hsu, N.C., Zhao, M., 2012. Global-scale attribution of anthropogenic and natural dust sources and their emission rates based on MODIS Deep Blue aerosol products. Rev. Geophys. 50. http://dx.doi.org/10.1029/2012RG000388.

Glamoclija, M., Fogel, M.L., Steele, A., Kish, A., 2012. Microbial nitrogen and sulfur cycles at the gypsum dunes of White Sands National Monument, New Mexico. Geomicrobiol J. 29, 733–751.

Ham, W.E., 1962. Economic geology and petrology of gypsum and anhydrite in Blaine County. Oklahoma Geol. Surv. Bull. 89, <http://www.ogs.ou.edu/pubsscanned/BULLETINS/Bulletin89.pdf>.

Hamdi-Aissa, B., Valles, V., Aventurier, A., Ribolzi, O., 2004. Soils and brine geochemistry and mineralogy of hyperarid desert playa, Ouargla Basin, Algerian Sahara. Arid Land Res. Manage. 18, 103–126.

Hand, J.L., Copeland, S.A., Day, D.E., Dillner, A.M., Indresand, H., Malm, W.C., McDade, C.E., Moore, C.T., Pitchford, M.L., Schichtel, B.A., Watson, J.G., 2011. Spatial and Seasonal Patterns and Temporal Variability of Haze and its Constituents in the United States: Report V. <http://vista.cira.colostate.edu/improve/Publications/Reports/2011/2011.htm>.

Hogan, J.F., Phillips, F.M., Mills, S.K., Hendrikx, J.M.H., Ruiz, J., Chesley, J.T., Asmerom, Y., 2007. Geologic origins of salinization in a semi-arid river: the role of sedimentary basin brines. Geology 35, 1063–1066.

Huneeus, N., Schulz, M., Balkanski, Y., Griesfeller, J., Prospero, J., Kinne, S., Bauer, S., Boucher, O., Chin, M., Dentener, F., Diehl, T., Easter, R., Fillmore, D., Ghan, S., Ginoux, P., Grini, A., Horowitz, L., Koch, D., Krol, M.C., Landing, W., Liu, X., Mahowald, N., Miller, R., Morcrette, J.-J., Myhre, G., Penner, J., Perlwitz, J., Stier, P., Takemura, T., Zender, C.S., 2011. Global dust model intercomparison in AeroCom phase I. Atmos. Chem. Phys. 11, 7781–7816.

Hyslop, N.P., White, W.H., 2008. An evaluation of Interagency Monitoring of PROtected Visual Environments (IMPROVE) collocated precision and uncertainty estimates. Atmos. Environ. 42, 2691–2705.

Hyslop, N.P., White, W.H., 2009. Estimating precision using duplicate measurements. J. Air Waste Manage. Assoc. 59, 1032–1039.

Hyslop, N.P., White, W.H., 2011. Identifying sources of uncertainty from the inter-species covariance of measurement errors. Environ. Sci. Technol. 45, 4030–4037.

Hyslop, N.P., Trzepla, K., White, W.H., 2012. Reanalysis of archived IMPROVE $PM_{2.5}$ samples previously analyzed over a 15-year period. Environ. Sci. Technol. 46, 10106–10113.

Ichikuni, M., Musha, S., 1978. Partition of strontium between gypsum and solution. Chem. Geol. 21, 359–363.

Jerolmack, D.J., Reitz, M.D., Martin, R.L., 2011. Sorting out abrasion in a gypsum dune field. J. Geophys. Res. 116. http://dx.doi.org/10.1029/2010JF001821.

Kavouras, I.G., Etyemezian, V., DuBois, D.W., Xu, J., Pitchford, M., 2009. Source reconciliation of atmospheric dust causing visibility impairment in Class I areas of the western United States. J. Geophys. Res. 114. http://dx.doi.org/10.1029/2008JD009923.

KellerLynn, K., 2012. White Sands National Monument: Geologic Resources Inventory Report. Natural Resource Report NPS/NRSS/GRD/NRR–2012/585. National Park Service, Fort Collins, Colorado, USA.

Kocurek, G., Carr, M., Ewing, R., Havholm, K.G., Nagar, Y.C., Singhvi, A.K., 2007. White Sands Dune Field, New Mexico: age, dune dynamics and recent accumulations. Sed. Geol. 197, 313–331.

Kok, J.F., 2011. A scaling theory for the size distribution of emitted dust aerosols suggests climate models underestimate the size of the global dust cycle. Proc. Natl. Acad. Sci. 108, 1016–1021.

Kushnir, J., 1980. The coprecipitation of strontium, magnesium, sodium, potassium and chloride ions with gypsum. An experimental study. Geochim. Cosmochim. Acta 44, 1471–1482.

Langford, R.P., 2003. The Holocene history of the White Sands dune field and influences on eolian deflation and playa lakes. Quatern. Int. 104, 31–39.

Langford, R.P., Rose, J.M., White, D.E., 2009. Groundwater salinity as a control on development of eolian landscape: an example from the White Sands of New Mexico. Geomorphology 105, 39–49.

Langner, J., Rodhe, H., Crutzen, P.J., Zimmerman, P., 1992. Anthropogenic influence on the distribution of tropospheric aerosol. Nature 359, 712–716.

Lowenthal, D., Kumar, N., 2006. Light scattering from sea-salt aerosols at IMPROVE sites. J. Air Waste Manage. Assoc. 56, 636–642.

Malm, W.C., Sisler, J.F., Huffman, D., Eldred, R.A., Cahill, T.A., 1994. Spatial and seasonal trends in particle concentration and optical extinction in the United States. J. Geophys. Res. 99, 1347–1370.

Malm, W.C., Pitchford, M.L., McDade, C., Ashbaugh, L.L., 2007. Coarse particle speciation at selected locations in the rural continental United States. Atmos. Environ. 41, 2225–2239.

Millero, F.J., 2004. Physicochemical controls on seawater. In: Holland, H.D., Turekian, K.K. (Eds.), Treatise on Geochemistry. Elsevier, Amsterdam (Chapter 6.01).

Neff, J.C., Reynolds, R.L., Munson, S.M., Fernandez, D., Belnap, J., 2013. The role of dust storms in total atmospheric particle concentrations at two sites in the western U.S.. J. Geophys. Res. 118, 11201–11212.

Novlan, D.J., 2011. Weather Forecast Manual,, .. White Sands Missile Range, fourth ed. Forecast Section, Meteorology Branch, White Sands Missile Range, New Mexico.

Park, S.H., Gong, S.L., Gong, W., Makar, P.A., Moran, M.D., Zhang, J., Stroud, C.A., 2010. Relative impact of windblown dust versus anthropogenic fugitive dust in $PM_{2.5}$ on air quality in North America. J. Geophys. Res. 115. http://dx.doi.org/10.1029/2009JD013144.

Pelletier, J.D., 2006. Sensitivity of playa windblown-dust emissions to climatic and anthropogenic change. J. Arid Environ. 66, 62–75.

Playa, E., Rosell, L., 2005. The celestite problem in gypsum Sr geochemistry: an evaluation of purifying methods of gypsiferous samples. Chem. Geol. 221, 102–116.

Reynolds, R.L., Yount, J.C., Reheis, M., Goldstein, H., Chavez Jr., P., Fulton, R., Whitney, J., Fuller, C., Forester, R.M., 2007. Dust emission from wet and dry playas in the Mojave Desert, USA. Earth Surf. Proc. Land. 32, 1811–1827.

Rogash, J., Hardiman, M., Novlan, D., Brice, T., MacBlain, V., 2009. Meteorological aspects of the 2006 El Paso Texas metropolitan area floods. Natl. Weather Digest 33, 77–101.

Rosell, L., Orti, R., Kasprzyk, A., Playa, E., Peryt, T.M., 1998. Strontium geochemistry of Miocene primary gypsum: Messinian of southeastern Spain and Cicily and Badenian of Poland. J. Sediment. Res. 68, 63–79.

Sanchez, M.L., Dominguez, J., Rodriguez, R., 2000. Aerosols in a Mediterranean forest: sulfates, particle size distribution, and growth rates. J. Air Waste Manage. Assoc. 50, 85–93.

Savage, K.B., 1981. Dispersion Modelling of Texas High Plains Duststorms. M.S. Thesis (Chemical Engineering), Texas Tech University, 146 pp.

Scheidt, S., Ramsey, M., Lancaster, N., 2010. Determining soil moisture and sediment availability at White Sands Dune Field, New Mexico, from apparent thermal inertia data. J. Geophys. Res. 115. http://dx.doi.org/10.1029/2009JF001378.

Schenk, C.J., Fryberger, S.G., 1988. Early diagenesis of eolian dune and interdune sands at White Sands, New Mexico. Sed. Geol. 55, 109–120.

Schutz, L., Sebert, M., 1987. Mineral aerosols and source identification. J. Aerosol Sci. 18, 1–10.

Sinclair, P.C., 1969. General characteristics of dust devils. J. Appl. Meteorol. 8, 32–45.

Smith, D.B., Cannon, W.F., Woodruff, L.G., Solano, F., Kilburn, J.E., Fey, D.L., 2013. Geochemical and Mineralogical Data for Soils of the Conterminous United States. Data Series 801, U.S. Geological Survey. Report (19 p) is at <http://pubs.usgs.gov/ds/801/>; data are in <http://pubs.usgs.gov/ds/801/downloads/Appendix_2b_Top5_18Sept2013.txt>.

Stewart, F.H., 1964. Marine Evaporites. Geological Survey Professional Paper 440-Y. <http://pubs.usgs.gov/pp/0440y/report.pdf>.
Szynkiewicz, A., Ewing, R.C., Moore, C.H., Glamoclija, M., Bustos, D., Pratt, L.M., 2010. Origin of terrestrial gypsum dunes—implications for martian gypsum-rich dunes of Olympia Undae. Geomorphology 121, 69–83.
Warren, J.K., 2006. Evaporites: Sediments, Resources and Hydrocarbons. Springer-Verlag, Berlin.
West, I., 1973. Vanished evaporites – significance of strontium minerals. J. Sediment. Petrol. 43, 278–279.
White, W.H., 2008. Chemical markers for sea salt in IMPROVE aerosol data. Atmos. Environ. 42, 261–274.
White, W.H., 2009. Considerations in the use of ozone and $PM_{2.5}$ data for exposure assessment. Air Qual. Atmos. Health 2, 223–230.
Wilson, J.C., McMurry, P.H., 1981. Studies of aerosol formation in power plant plumes – II. Secondary aerosol formation in the Navajo Generating Station plume. Atmos. Environ. 15, 2329–2339.